EUROPEAN ORGANIZATION FOR NUCLEAR RESEARCH

CERN-EP/85-186
14 November 1985

HIGH-p_T $\alpha\alpha$ AND αp INTERACTIONS

W. Bell[1], K. Braune[2a], G. Claesson[3b], D. Drijard[1], M.A. Faessler[1], H.G. Fischer[1], H. Frehse[1c], R.W. Frey[4d], S. Garpman[3], W. Geist[1b], C. Gruhn[5], P. Hanke[6], M. Heiden[1b], W. Herr[6], P.G. Innocenti[1], T.J. Ketel[2e], E.E. Kluge[6], I. Lund[3], G. Mornacchi[1], T. Nakada[6d], I. Otterlund[3], M. Panter[1], B. Povh[2], A. Putzer[6], E. Stenlund[3], T.J.M. Symons[5], R. Szwed[2f] and O. Ullaland[1]

(CERN-Heidelberg-Lund Collaboration)

ABSTRACT

Properties of secondaries associated with a high-p_T charged trigger particle ($3 < p_T < 5$ GeV/c) were studied for αp and $\alpha\alpha$ interactions at c.m. energies $\sqrt{s} = 88$ GeV and 125 GeV, respectively. The p_T distributions of secondaries in the away-jet and trigger-jet regions were compared with those for high-p_T pp interactions. No statistically significant differences were seen, except at low p_T. Momentum and angular distributions of spectator and leading protons were studied as a function of charge and rapidity of the trigger hadron. The observed correlations between trigger charge and number of spectator protons provide evidence of valence quark contributions to the trigger jet.

(Submitted to Zeitschrift für Physik C)

---

1) CERN, Geneva, Switzerland.
2) Max-Planck Institut für Kernphysik, Heidelberg, Fed. Rep. Germany.
3) Division of Cosmic and Subatomic Physics, University of Lund, Sweden.
4) Physikalisches Institut der Universität, Heidelberg, Fed. Rep. Germany.
5) Nuclear Science Division, Lawrence Berkeley Laboratory, Berkeley, Calif., USA.
6) Institut für Hochenergiephysik der Universität Heidelberg, Fed. Rep. Germany.

[a] Present address: CERN, Geneva, Switzerland.
[b] Present address: LBL, Berkeley, USA.
[c] Present address: Control Data Corporation, Zurich, Switzerland.
[d] Present address: SIN, Villigen, Switzerland.
[e] Present address: Natuurkundig Lab., Vrije Universiteit, Amsterdam, The Netherlands.
[f] On leave from the Inst. of Exp. Physics, University of Warsaw, Poland.

1. INTRODUCTION

The subject of high-p_T hadron production from nuclei attracted wide interest when the Chicago–Princeton group of FNAL [1], and later other experiments [2], found that the yield of hadrons at transverse momentum $p_T > 2$ GeV/c grows faster than linearly with the nucleon number A of the target.

One of the hypotheses to explain this 'anomalous nuclear enhancement' was that the parton, leading to the large-p_T trigger hadron, rescattered from different nucleons in the target nucleus [3]. This mechanism implies that instead of one away jet, two or more jets would balance the p_T of the trigger jet, hence the momentum distribution of particles opposite the trigger would be expected to soften.

The potential role of the Fermi motion of nucleons has often been discussed. The intrinsic transverse momentum of nucleons may help to boost the p_T of the trigger (as does the primordial transverse momentum k_T of the partons) and their intrinsic longitudinal momentum may lead to larger-than-average centre-of-mass (c.m.) energy $\sqrt{s_{NN}}$ of the nucleon–nucleon collisions. The distribution of spectator fragments contains, in principle, the information about the role of the Fermi motion.

The already published [4–6] inclusive cross-sections measured as a function of p_T in $p\alpha$ and $\alpha\alpha$ interactions at the CERN Intersecting Storage Rings (ISR) are consistent with extrapolations from FNAL results, although there are indications from one of the ISR experiments [7] that in $p\alpha$ interactions the inclusive cross-section at $p_T > 5$ GeV/c is lower than expected and in $\alpha\alpha$ interactions it is higher.

In the present letter we examine the role of the nuclear environment in hard interactions by studying the properties of particles produced together with the large-p_T trigger hadron in $\alpha\alpha$ and αp interactions. After a short description of the apparatus and analysis (Section 2), we show and compare, in Section 3, particles produced in the central rapidity region, i.e. the trigger and away-jet region. In Section 4 we concentrate on the spectrum of spectator and leading protons emitted from the α-particle.

2. EXPERIMENT AND ANALYSIS

The experiment was performed with the Split-Field Magnet (SFM) detector at the CERN ISR at c.m. energies $\sqrt{s} = 88$ GeV for αp and $\sqrt{s} = 125$ GeV for $\alpha\alpha$ collisions. The results for the inclusive cross-section of the trigger hadron as a function of p_T have already been published [5]; the apparatus and some details of the triggering procedure were described in that paper.

The trigger required a single, charged, high-p_T n in one of two independent trigger regions with polar angles θ of approximately 45° with respect to the incoming beams; both regions were around the horizontal plane defined by the intersecting beams [azimuthal angle $|\phi(\text{tri})| < 10°$]. The present study is based on samples of fully reconstructed events where the p_T of the trigger particle, $p_T(\text{tri})$, was larger than 3 GeV/c. This lower p_T cut-off was applied because at this value the anomalous nuclear enhancement is already well developed at FNAL energies for pA collisions, i.e. the power $\alpha(p_T)$ of the A dependence has almost reached its highest value of 1.15 for pions [1]. The range and average values of the kinematic variables for the trigger track are listed in Table 1a for the different event samples used for this work. Pion identification was possible in the high-p_T trigger region for total laboratory momenta from 3.8 to 5.5 GeV/c, using two threshold Cherenkov counters filled with freon-12. The total number of all events, of events with a positively or negatively charged trigger hadron, h^- or h^+, and of those with identified trigger hadrons (pions versus non-pions, i.e. K or p) are given in Table 1b. If not explicitly mentioned all quantities are given in the nucleon–nucleon (NN) c.m. system (neglecting Fermi motion). For the case of αp interactions, it is important to note that according to our convention

the incoming α has positive longitudinal momentum p_L or rapidity y; since the beam momenta in the laboratory system are asymmetric (31 GeV/c protons on 62 GeV/c alphas), the two y(tri) windows, which are mirror symmetric for $\alpha\alpha$ and pp, are asymmetric in the c.m. system for $p\alpha$. For comparison we will also refer to 'minimum bias events' with the only trigger requirement being at least one charged track anywhere in the central rapidity region $|y| < 2$.

The SFM detector covers a solid angle of almost 4π for momentum measurement of charged particles. Owing to the magnetic field geometry and chamber arrangements, the momentum resolution varies as a function of angle, charge, and momentum of the tracks. For the analysis described here, only tracks with an estimated momentum resolution $\Delta p/p < 0.3$ were accepted. The shown distributions are corrected for acceptance.

3. THE CENTRAL RAPIDITY REGION

The approximate planarity of the high-p_T events and the ϕ dependence of the momentum resolution of the detector leads us to select, for particles produced in the central rapidity region $|y| < 2$, two $\Delta\phi$ wedges which are defined by the cuts:

$$\begin{aligned} \Delta\phi &= |\phi - \phi(\text{tri})| < 35^\circ \text{ ('towards')} , \\ \Delta\phi &= |\phi - \phi(\text{tri})| > 145^\circ \text{ ('away')} , \end{aligned} \tag{1}$$

where 'towards' refers to particles going to the same ϕ hemisphere as the trigger particle, and 'away' refers to particles recoiling against the trigger hadron.

As already shown in a previous paper by the Axial-Field Spectrometer (AFS) Collaboration [6], the shape of the ϕ distributions for high-p_T $\alpha\alpha$ events is similar to that for pp interactions, displaying enhancements around $\Delta\phi = 0$ and $\Delta\phi = 180^\circ$ which increase and become narrower with increasing p_T of the secondaries. These enhancements are attributed to the trigger jet and the away jet, respectively. [Note that for $\alpha\alpha$ interactions, the away-side enhancement seems somewhat wider in ϕ than for pp interactions (see Fig. 6 of Ref. [6]). Such a feature is expected from parton rescattering processes leading to more than one away jet; thus the observed widening may be considered as an indication that such processes do take place. Note also that the pedestals below the enhancements increase when going from pp to $\alpha\alpha$ interactions, and can probably be explained by a higher background of particles which are not directly associated with the towards and away jets.]

Given the ϕ distributions as measured by the AFS Collaboration, it is obvious that our $\Delta\phi$ cuts are somewhat arbitrary with respect to the containment of the away and trigger jets. However, since our aim is to measure ratios between the distributions of jet-associated particles for $\alpha\alpha$, αp, and pp interactions rather than absolute distributions, the choice of this cut is not critical.

The main result of this section concerns the p_T and x_E distributions of associated secondaries within the towards and away $\Delta\phi$ wedges and within a rapidity window $|y| < 2$. Before we come to these distributions, we show another projection of the particle distribution in momentum space which, together with the projection on the ϕ coordinate (Fig. 6 of Ref. [6]), illustrates the general structure of the high-p_T events: Fig. 1 displays the average rapidity distribution dn/dy (normalized to one event) for secondaries with p_T larger than 1 GeV/c in both $\Delta\phi$ wedges. (The trigger particle is neither included in these distributions nor in any following distribution.) In these plots we make a comparison with the corresponding distributions for minimum-bias events. The prominent features of the high-p_T events, compared with low-p_T events, are the significant increase of associated secondaries on the away side over a wide rapidity interval (about $|y| < 2$) and, on the towards side, the narrow enhancement around the trigger-particle rapidity; this is

particularly true for secondaries with larger-than-average p_T, which was the reason for choosing a p_T cut of 1 GeV/c for this plot. These features are already well known from pp interactions.

In the case of αp interactions, the trigger-side enhancements are very similar to those in the corresponding pp interactions. For $\alpha\alpha$ interactions the enhancement is less significant; within the statistical errors of the data points the change of the towards-side structure in $\alpha\alpha$ compared with αp interactions can presumably be explained by the expected [8] higher trigger-bias which has been measured for pp interactions [9]. ['Trigger bias' refers to the observation that a high-p_T single-particle trigger favours jets where one hadron—the trigger particle—carries a particularly high fraction of jet momentum. This bias increases with increasing $x_T = 2\,p_T(\mathrm{tri})/\sqrt{s_{NN}}$].

Turning to the transverse momentum spectrum of associated secondaries in the central rapidity region, we show first the p_T distribution dn/dp_T for $|y| < 2$ and within the two $\Delta\phi$ wedges for the data samples 1, 3, and 4 (Fig. 2). For comparison, the p_T distribution in minimum-bias αp events is indicated as well. The distributions for the three large-p_T samples are rather similar; on the away side (positive p_T) they fall off much less rapidly than the one for minimum-bias events. On the towards side (negative values of p_T) the distributions are steeper, and those for large-p_T events are closer to the ones for minimum-bias triggers.

We now compare p_T distributions in the region of the away jet(s) (away side) and of the trigger jet (towards side) for αp and $\alpha\alpha$ interactions with pp interactions [10]. The goals are: i) to study whether, and to what extent, the momentum spectrum on the away side softens for $\alpha\alpha$ and αp interactions as implied by parton rescattering models; ii) to search for eventual changes of the structure of the trigger jet. For the purpose of comparison, we replace the variable p_T by the scaling variable

$$x_E = - \vec{p}_T \vec{p}_T(\mathrm{tjet})/|\vec{p}_T(\mathrm{tjet})|^2 \ , \tag{2}$$

where $\vec{p}_T(\mathrm{tjet})$ signifies the p_T of the trigger jet. The advantage of using x_E is that effects of different trigger p_T—and, moreover, for the away-side comparison, the effects of different trigger biases—are minimized. (For the comparison of αp with pp the use of x_E instead of p_T is not essential, since in this case we will compare data samples with equal ranges and average values of p_T and with equal $\sqrt{s_{NN}}$.) In order to calculate x_E one needs to know $p_T(\mathrm{tjet})$. Results from the CDHW Collaboration [9] show that the average ratio of the trigger particle momentum to the trigger jet momentum,

$$\langle z \rangle = \langle p_T(\mathrm{tri})/p_T(\mathrm{tjet}) \rangle \ , \tag{3}$$

is a function of $x_T = 2\,p_T/\sqrt{s}$, in agreement with QCD predictions. [This ratio $\langle z \rangle$ is a measure of the already mentioned 'trigger bias'.] For x_T varying from 0.11 to 0.23, $\langle z \rangle$ varies from 0.75 to 0.82. Owing to the limited statistics of our $\alpha\alpha$ and αp data we cannot determine $\langle z \rangle$ self-consistently by applying the procedure of Ref. [9]; therefore we use the data of Ref. [9] to obtain $p_T(\mathrm{tjet})$ from $p_T(\mathrm{tri})$ on an event-by-event basis and are thus able to calculate x_E, assuming that the jet direction is the same as the trigger particle direction.

In Fig. 3 we show the ratio

$$R_{XE}(\alpha p/pp) = [dn/dx_E(\alpha p)]/[dn/dx_E(pp)] \tag{4}$$

and, correspondingly, $R_{XE}(\alpha\alpha/pp)$; the pp data used for this comparison were taken with the same apparatus and the same trigger by the CDHW Collaboration [10]. The ratios $R_{XE}(\alpha p/pp)$ are somewhat larger than 1 for small x_E and decrease slightly for increasing positive x_E (away

side). On the towards side a decrease of the ratio may be indicated (Fig. 3a) but the errors are large. For $R_{XE}(\alpha\alpha/pp)$ the ratio is higher than 1 at low x_E and decreases on both the towards and the away side for increasing $|x_E|$. A similar result was obtained by the AFS Collaboration comparing x_E distributions for $\alpha\alpha$ with those for pp interactions ($\sqrt{s}$ = 31 GeV) (see Fig. 5 of Ref. [6]).

The rise of R_{XE} above 1 at low x_E has probably to be attributed to non-jet-associated particles in high-p_T events. (A similar rise has been observed comparing normal inelastic, i.e. minimum-bias, events from $\alpha\alpha$ and αp, with pp interactions [11].) To be free from these 'background' particles, i.e. to compare only jet-associated particles, one should consider the ratio only at large x_E. The away-side ratios at large x_E ($x_E > 0.4$) show that the x_E distributions in $\alpha\alpha$, αp, and pp interactions are consistent with each other within our statistical errors. Let us recall that we studied these ratios to obtain information on multiple parton scattering or parton rescattering in high-p_T production from nuclei. No quantitative predictions on the change of the x_E distributions are available, but a simple estimate can be performed assuming that for such processes two or more away jets recoil against the trigger jet. Hence the away-side x_E distribution should fall more steeply than it would for events without rescattering. The deviation of the ratios R_{XE} from 1 at high x_E is a direct measure of the relative increase of these processes. Thus we find that it is not excluded that parton rescattering in αp and $\alpha\alpha$ occurs on a level up to 20% and 40% for αp and $\alpha\alpha$, respectively.

The decrease of the ratio on the towards side (negative x_E) for $\alpha\alpha$ interactions (Fig. 3c) may be, at least in part, explained by the already mentioned higher trigger bias. The small and statistically not very significant difference between the α-side and p-side jets in αp interactions as displayed by the towards-side ratios (Fig. 3a,b) is probably linked to the earlier published observation that the inclusive cross-section $d\sigma/dp_T^2$ on the α-side decreases more quickly than the one on the p-side [5]. It is not clear whether this difference between α-side and p-side triggers is due to the difference in the absolute values of $\langle y(tri)\rangle$ (see Table 1) or to the fact that one jet emerges from the alpha, the other one from the proton.

4. THE NUCLEAR SPECTATOR REGION

The unique combination of the special features of the SFM detector and of the general properties of the α-particle interactions allowed us to measure the spectrum of non-pair-produced protons over a range of Feynman $x_F = 2p_L/\sqrt{s_{NN}}$ from about 0.1 to 1.4. Firstly, since the α-beam rigidity was 62/Q = 31 GeV/c per charge, charged particles with 0 angle and momenta up to 20 GeV/c are bent out of the beam pipe by the dipole fields and are seen by the detector; only above 20 GeV/c is the acceptance zero for p_T below a p_L-dependent cut-off value owing to the beam pipe geometry. Secondly, since the reactions $n \rightarrow \pi^{\pm}$ and $p \rightarrow \pi^{\mp}$ are isospin symmetric and the α particle has isospin 0, the π^+ and π^- yields for $\alpha\alpha$ interactions are equal everywhere in momentum. Thus by forming the difference between positive and negative particles, $dn_+/dp_L - dn_-/dp_L$, one expects to obtain the spectrum of non-pair-produced protons if the difference between K^+ and K^- yields is neglected. For αp interactions these arguments are only valid on the α side (positive p_L, according to our definition).

In previous publications we have shown the spectrum of protons for quasi-elastic interactions [12] and for normal inelastic interactions [11], and we have also examined the dependence of the proton spectrum on the multiplicity of produced particles [11]. Here we will consider the invariant distribution

$$E(dn_+/dp_L - dn_-/dp_L) \qquad (5)$$

for various trigger conditions. The proton mass was used to calculate the energy E. In Fig. 4 this distribution is shown for minimum-bias events and for four classes of high-p_T events: positive and negative trigger charge, and trigger in the same or the opposite polar hemisphere with respect to the α particle.

Comparing the distributions (histograms) for high-p_T events with those for minimum-bias events (smooth curve), one notices changes at low and high p_L. Most prominent is the decrease of the spectator peak at $+15$ GeV/c for the case of a positively charged high-p_T trigger particle at positive p_L (Figs. 4c and 4e). In all other cases (trigger charge negative, or the sign of the trigger p_L opposite to that of the spectator p_L) the spectator peak is either larger than or consistent with the one in minimum-bias events. The energy contained in the spectator peak, i.e. the integral

$$\int_{13}^{20} E(dn_+/dp_L - dn_-/dp_L)\, dp_L \ , \tag{6}$$

is shown in Table 2 for various data samples (the lower integration limit $p_L = 13$ GeV/c is somewhat arbitrary). The average energy of the trigger hadrons in the reference systems chosen for Fig. 4, and for the different event samples, was between 4.3 and 4.5 GeV/c.

The effect, displayed in Fig. 4, of a long-range (in y or p_L) correlation depends apparently mainly on the charge, since a further division into subsamples belonging to identified trigger hadrons (π or K + p), does not show any statistically significant differences. Here we only mention, without illustrating, that no charge correlations are observed if (off-line) a low-p_T trigger hadron is required within the same rapidity windows as the high-p_T trigger hadron. (However, one expects to see a similar effect if one selects events with a low-p_T secondary having an energy comparable to that of the high-p_T trigger hadron; this test has yet to be done.)

The observed long-range correlation in p_L between the charge of the high-p_T trigger hadron and the number of spectator protons (or the energy carried by the latter) can be qualitatively explained by assuming that valence quarks of the incoming α particle go into the trigger hadron. Thus, if the trigger hadron were positive and went into the same hemisphere as the α, it would be more likely that a proton out of the α particle interacted, depleting the number of non-interacting (i.e. spectator) protons. If the trigger hadron were negative (i.e. a π^-, since K^- and $\bar{p}$ are entirely made of sea quarks), it would be more likely that a neutron interacted. This should leave more spectator protons than for minimum-bias events, since, for the latter, the average number of interacting neutrons and protons should be equal. For trigger hadrons on the side opposite to the α particle, no (or a weaker) correlation is expected (and seen) because partons out of the other α particle (for $\alpha\alpha$ collisions) or out of the proton (for $p\alpha$) contribute to them.

A quantitative interpretation would require a comparison with QCD calculations of all the cross-sections $\sigma(p,n \rightarrow \pi^+, \pi^-, K^+, K^-, p, \bar{p})$, and it is obscured by the fact that not all spectator protons are seen because some of them are carried away in heavier fragments (d, t, ^{3}He) which are mostly undetected in the present set-up. In reference [11] it was shown that the number of missing protons (on one α side) varies from 1, for very low multiplicity $\alpha\alpha$ interactions, to 0, for very high multiplicity events. For high-p_T events these numbers may be somewhat different.

Contributions of the transverse Fermi motion of nucleons to the trigger p_T should show up as a recoil of spectator protons. In order to display such effects, the distribution of spectator protons in azimuthal angle and in p_T was investigated.

In Fig. 5 we show the ϕ distribution $dn/d\phi$ of spectator protons, defined as an excess of positive particles in the p_L range $13 < p_L < 20$ GeV/c, in high-p_T events divided by the distribution in minimum-bias events. An asymmetry of $dn/d\phi$ would be the most direct sign for an active role of the transverse Fermi motion in high-p_T events. The division by $dn/d\phi$ for

minimum-bias events (uniform ϕ distribution of protons) was done in order to eliminate structures of the ϕ distribution which result from non-uniform detector acceptance. In Fig. 6 the ratios of the p_T distributions dn/dp_T are shown for spectators in the azimuthal hemisphere opposite to the trigger hadron. The distribution dn/dp_T^2 for minimum-bias events, corresponding to the denominator of the dn/dp_T ratio, was shown in reference [11]. A deviation of this ratio from 1 is expected if a small recoil momentum is added to the spectator p_T .

In both cases the ratios are consistent with 1 for all ϕ and p_T. Hence, within our statistical errors, we do not see any effect from transverse Fermi motion in these data samples. However, we should mention that investigations are being made on larger data samples (smaller statistical errors) for high-p_T $\alpha\alpha$ and dd collisions, obtained in a new run. If there is an effect from the longitudinal Fermi momentum which would increase the effective $\sqrt{s_{NN}}$ to above average for certain NN collisions, this effect would show up as a shift of spectator particles to lower p_L, hardly distinguishable from a depletion as we see it in Figs. 4c and 4e. However, it would not depend on the trigger charge.

5. CONCLUSIONS

We made a precise comparison of x_E distributions of particles produced in the central region, opposite the trigger hadron, by αp and $\alpha\alpha$ interactions, with corresponding x_E distributions in pp interactions. Owing to statistical errors the comparison does not prove the hypothesis of multiple hard-parton interactions, but it allows for such mechanisms up to a level of 20% in αp and 40% in $\alpha\alpha$ interactions.

The results of the study of the number of spectator protons and their distributions in high-p_T $\alpha\alpha$ and αp interactions do not support any important role of nuclear Fermi motion in the high-p_T production mechanism—for the given range of y and p_T of the trigger hadron and the given statistical errors of the data. However, the observed long-range correlations between the trigger hadron charge and the energy carried by spectator protons are evidence of valence quark contributions to the high-p_T trigger hadron. The measurement of the number of spectator protons is equivalent to having tagged proton and neutron beams. It is only because protons are lost if they are built into heavier fragments that this tagging is incomplete. For dd and dp collisions, using the same set-up, tagging can be improved.

Acknowledgements

The Heidelberg group was supported by a grant from the Bundesministerium für Forschung und Technologie of the Federal Republic of Germany. The Lund Group gratefully acknowledges financial support from the Swedish Natural Science Research Council. One of us (MAF) thanks the Deutsche Forschungsgemeinschaft for a Heisenberg Fellowship.

Table 1

Event samples

a) Kinematic range of the trigger hadron

Sample	Beams	$\sqrt{s_{NN}}$ (GeV)	p_T(tri) Range (GeV/c)	p_T(tri) Average	y(tri) Range	y(tri) Average
1	αα	31.2	3 to 5	3.39	0.5 to 1.0	0.73
2	αα	31.2	Minimum bias		−2.0 to 2.0	
3	αp	44.0	3 to 5	3.46	0.8 to 1.4	1.11
4	αp	44.0	3 to 5	3.50	−0.7 to −0.1	−0.4
5	αp	44.0	Minimum bias		−2.0 to 2.0	

b) Number of all events and of events with an identified trigger hadron

Sample	Events	h^+	h^-	π^+	π^-	$K^+ + p$	$K^- + \bar{p}$
1	916	386	530				
2	100000						
3	1890	756	1134	316	561	237	107
4	3960	1768	2192	703	827	498	338
5	37000						

Table 2

Energy of associated spectator protons

$\int_{13}^{20} E(dn_+/dp_L - dn_-/dp_L)\, dp_L$ in GeV

Sample	h^+	π^+	$K^+ + p$	h^-	π^-	$K^- + \bar{p}$
1[a]	4.2 ± 1.6			6.0 ± 1.0		
1[b]	9.4 ± 1.6			6.4 ± 0.9		
3	3.4 ± 0.5	3.1 ± 0.7	3.6 ± 0.8	7.8 ± 0.9	7.4 ± 1.3	10.4 ± 3.1
4	7.0 ± 0.6	6.0 ± 0.8	9.1 ± 1.6	7.1 ± 0.7	8.7 ± 1.6	5.7 ± 0.9
2	6.3 ± 0.1					
5	5.9 ± 0.2					

a) Trigger on same side as spectator proton (i.e. trigger and spectator p_L have same sign).

b) Trigger and spectator on opposite sides.

REFERENCES

[1] J.W. Cronin et al., Phys. Rev. **D11** (1975) 3105.
L. Kluberg et al., Phys. Rev. Lett. **38** (1977) 670.
D. Antreasyan et al., Phys. Rev. **D19** (1979) 764.

[2] U. Becker et al., Phys. Rev. Lett. **37** (1976) 1731.
D.A. Garbutt et al., Phys. Lett. **67B** (1977) 355.
R.L. Mac Carthy et al., Phys. Rev. Lett. **40** (1978) 213.
C. Bromberg et al., Phys. Rev. Lett. **42** (1979) 1202.

[3] J.H. Kühn, Phys. Rev. **D13** (1976) 2948.
P.M. Fishbane et al., Phys. Rev. **D16** (1977) 122.
A. Krzywicki et al., Phys. Lett. **85B** (1979) 407.
V.V. Zmushko, Sov. J. Nucl. Phys. **32** (1980) 127 and 231.
D. Treleani and G. Wilk, Nuovo Cimento **60A** (1980) 201.
U.P. Sukhatme and G. Wilk, Phys. Rev. **D25** (1982) 1978.
M. Lev and B. Peterson, Z. Phys. **21 (1983) 155.**

[4] A. Karabarbounis et al., Phys. Lett. **104B** (1981) 75.

[5] W. Bell et al., Phys. Lett. **112B** (1982) 271.

[6] T. Åkesson et al., Nucl. Phys. **209** (1982) 209.

[7] A.L.S. Angelis et al., Phys. Lett. **116B** (1982) 379.

[8] M. Jacob and P.V. Landshoff, Nucl. Phys. **B113** (1976) 395.

[9] C.D. Buchanan (CERN-Dortmund-Heidelberg-Warsaw Collaboration), Proc. 17th Rencontre de Moriond, Les Arcs, 1982, ed. J. Tran Thanh Van (Éditions Frontières, Gif-sur-Yvette, 1982), Vol. II, p. 139.
W. Geist, Invited talk at the Summer Institute on Particle Physics, Stanford, 1982, preprint CERN-EP/82-184 (1982).

[10] CERN-Dortmund-Heidelberg-Warsaw Collaboration (Exp. 416), unpublished data.

[11] W. Bell et al., Nucl. Phys. **B254** (1985) 475.

[12] W. Bell et al., Z. Phys. **C27** (1985) 191.

Figure captions

Fig. 1 Rapidity distributions of associated particles (trigger particle not included) with $p_T > 1$ GeV/c in the two $\Delta\phi$ wedges for a) αp sample 3, b) αp sample 4, c) $\alpha\alpha$ sample 1. Particles on the towards side are plotted with positive values of dn/dy, those on the away side with negative values. The rapidity distribution was shifted for each event by a small Δy ($|\Delta y| < 0.5$) in such a way as to have y(tri) at an exact position corresponding to $\langle y(tri)\rangle$. The location of the trigger hadron is indicated by an arrow. Small data points connected by histograms represent distributions for minimum-bias events (samples 2 and 5).

Fig. 2 Distribution in p_T of associated particles in the central region ($|y| < 2$) and in the two $\Delta\phi$ wedges (event samples 1, 3, and 4). Negative (positive) values of p_T correspond to tracks on the towards (away) side. The small data points represent the p_T distribution for αp minimum-bias events (sample 5).

Fig. 3 Ratio of x_E distributions [see definitions (2) and (4) in the text] on the towards side (negative x_E) and away side (positive x_E) in the central rapidity region $|y| < 2$: a) αp ($\langle y(tri)\rangle = 1.1$), b) αp ($\langle y(tri)\rangle = -0.4$), c) $\alpha\alpha$ interactions. For the denominator of the ratio, pp data taken by the CDHW Collaboration [10] were used.

Fig. 4 The invariant distribution $E(dn_+/dp_L - dn_-/dp_L)$ of the positive excess particles (dominantly protons) as a function of p_L. For $\alpha\alpha$ collisions, p_L is given in the c.m. system; for αp collisions, a reference system has been used where the α beam has the same momentum (15.6 GeV/c per nucleon) as for $\alpha\alpha$ collsions, the proton beam has 31.2 GeV/c, but α and p are made collinear. a) αp, b) $\alpha\alpha$ minimum-bias interactions. In (c) to (h) the corresponding distributions of associated particles are shown (histograms) and compared with minimum-bias events (continuous curve) for high-p_T $\alpha\alpha$ [(c) and (d)] and αp [(e) to (h)] interactions, for negative and positive charge (Q) and for negative and positive y or p_L of the trigger hadron. For $\alpha\alpha$ interactions, the two distributions for positive and negative p_L of the trigger have been superimposed by reflecting the latter distribution, and the histograms have been smoothed to reduce the statistical fluctuations.

Fig. 5 The azimuthal distribution $dn/d\phi$ of spectator protons ($13 < p_L < 20$ GeV/c, see previous figure) from the α particle, for high-p_T events divided by the corresponding distribution for minimum-bias events. a) and b) αp; c) and d) $\alpha\alpha$ interactions. In (a) and (c) the trigger hadron and spectator are in the same polar hemisphere (i.e. trigger p_L and spectator p_L have the same sign); for (b) and (d) they are in opposite hemispheres.

Fig. 6 The p_T distribution dn/dp_T of spectator protons (same p_L cut as for Fig. 2) in the azimuthal hemisphere opposite to the trigger hadron (i.e. $90° < |\phi(\text{proton})| < 180°$) for high-$p_T$ interactions divided by the corresponding distribution for minimum-bias interactions. a) to c) as in previous figure.

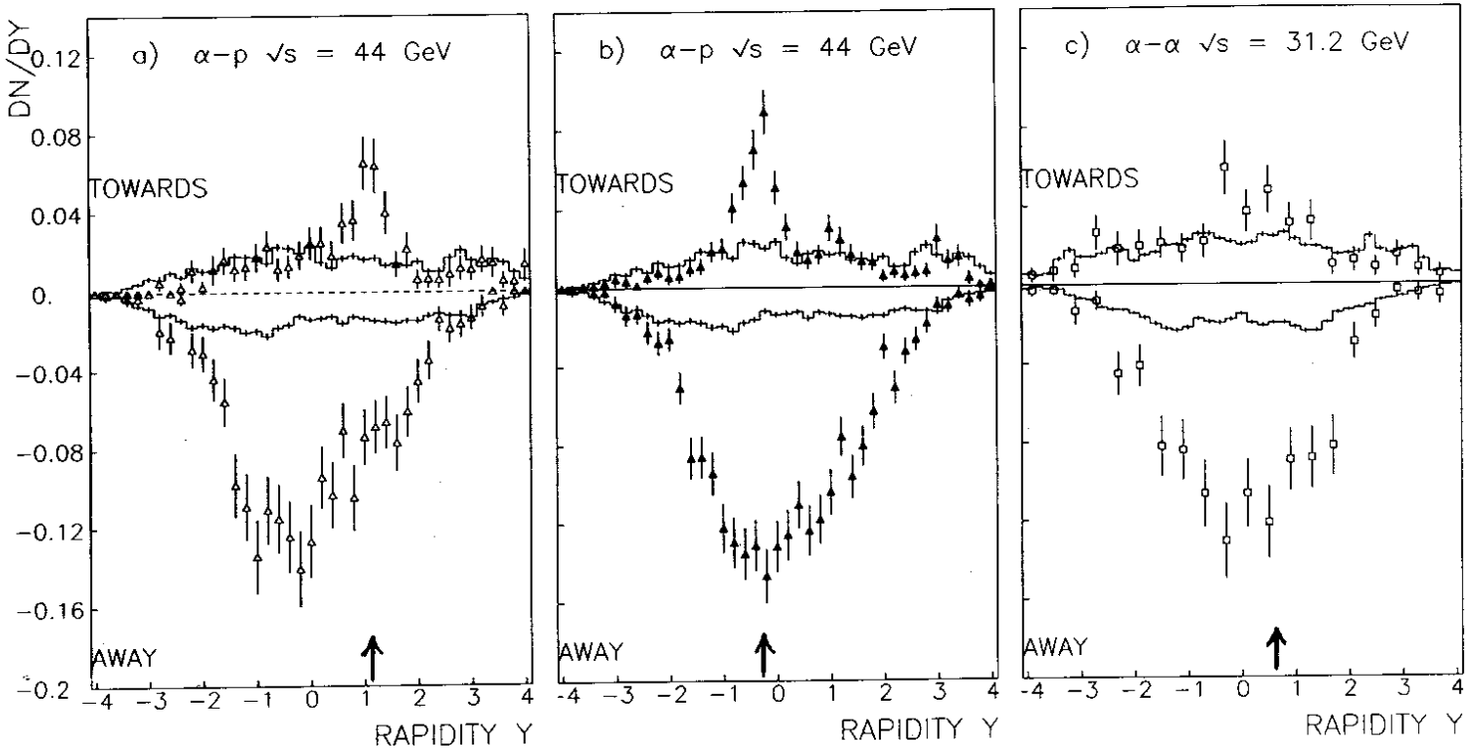
a) α−p √s = 44 GeV
b) α−p √s = 44 GeV
c) α−α √s = 31.2 GeV
DN/DY
TOWARDS
AWAY
RAPIDITY Y
0.12
0.08
0.04
0.
−0.04
−0.08
−0.12
−0.16
−0.2
−4 −3 −2 −1 0 1 2 3 4

Fig. 1

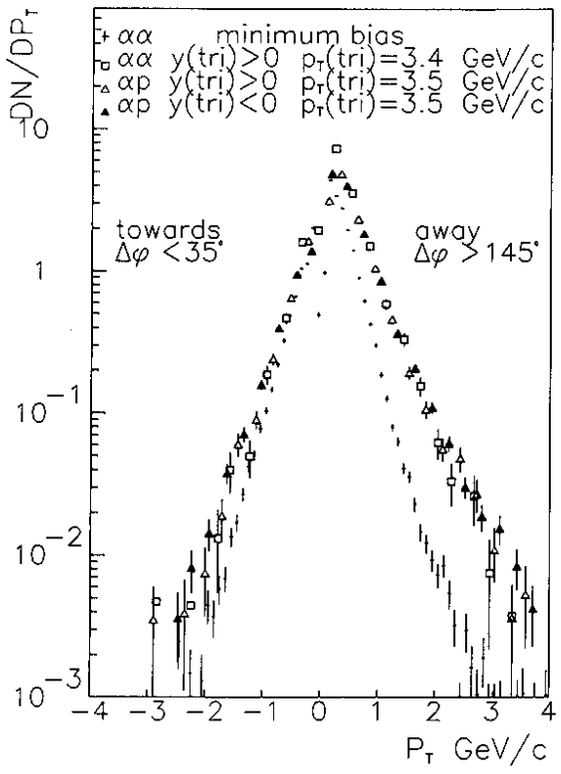
αα minimum bias
αα y(tri)>0 p_T(tri)=3.4 GeV/c
αp y(tri)>0 p_T(tri)=3.5 GeV/c
αp y(tri)<0 p_T(tri)=3.5 GeV/c
towards
Δφ <35°
away
Δφ >145°
DN/DP$_T$
P$_T$ GeV/c

Fig. 2

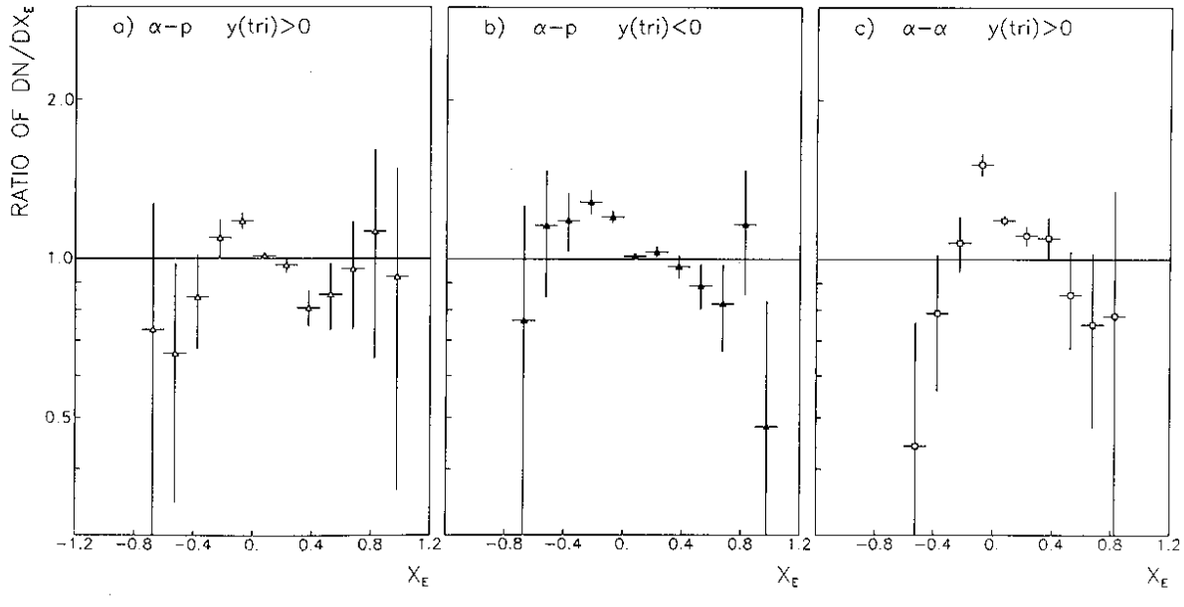
a) α−p y(tri)>0
b) α−p y(tri)<0
c) α−α y(tri)>0
RATIO OF DN/DX$_E$
X$_E$

Fig. 3

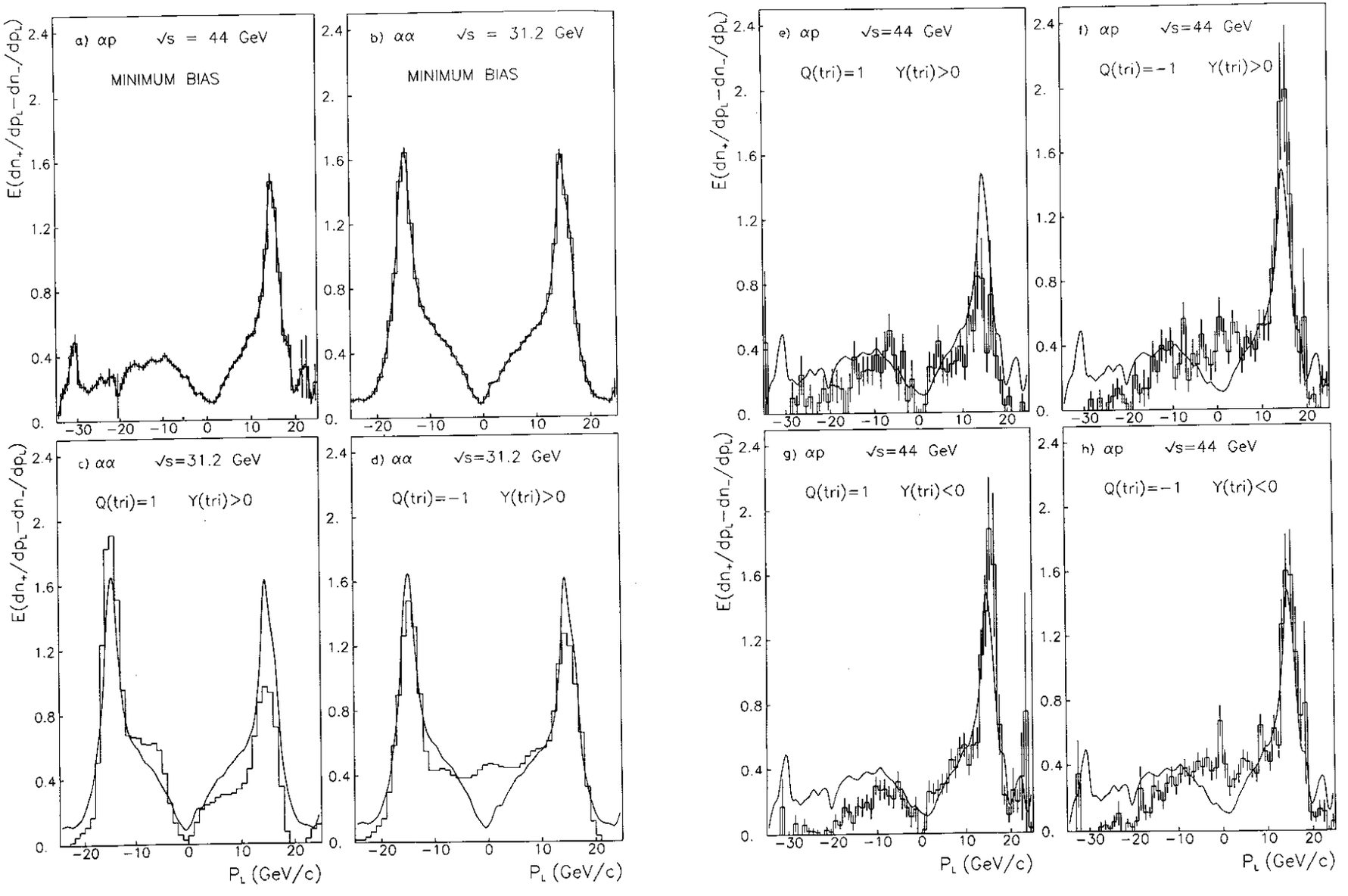
a) αp √s = 44 GeV
MINIMUM BIAS
b) αα √s = 31.2 GeV
MINIMUM BIAS
c) αα √s=31.2 GeV
Q(tri)=1 Y(tri)>0
d) αα √s=31.2 GeV
Q(tri)=−1 Y(tri)>0
e) αp √s=44 GeV
Q(tri)=1 Y(tri)>0
f) αp √s=44 GeV
Q(tri)=−1 Y(tri)>0
g) αp √s=44 GeV
Q(tri)=1 Y(tri)<0
h) αp √s=44 GeV
Q(tri)=−1 Y(tri)<0
E(dn+/dpL−dn−/dpL)
PL (GeV/c)

Fig. 4

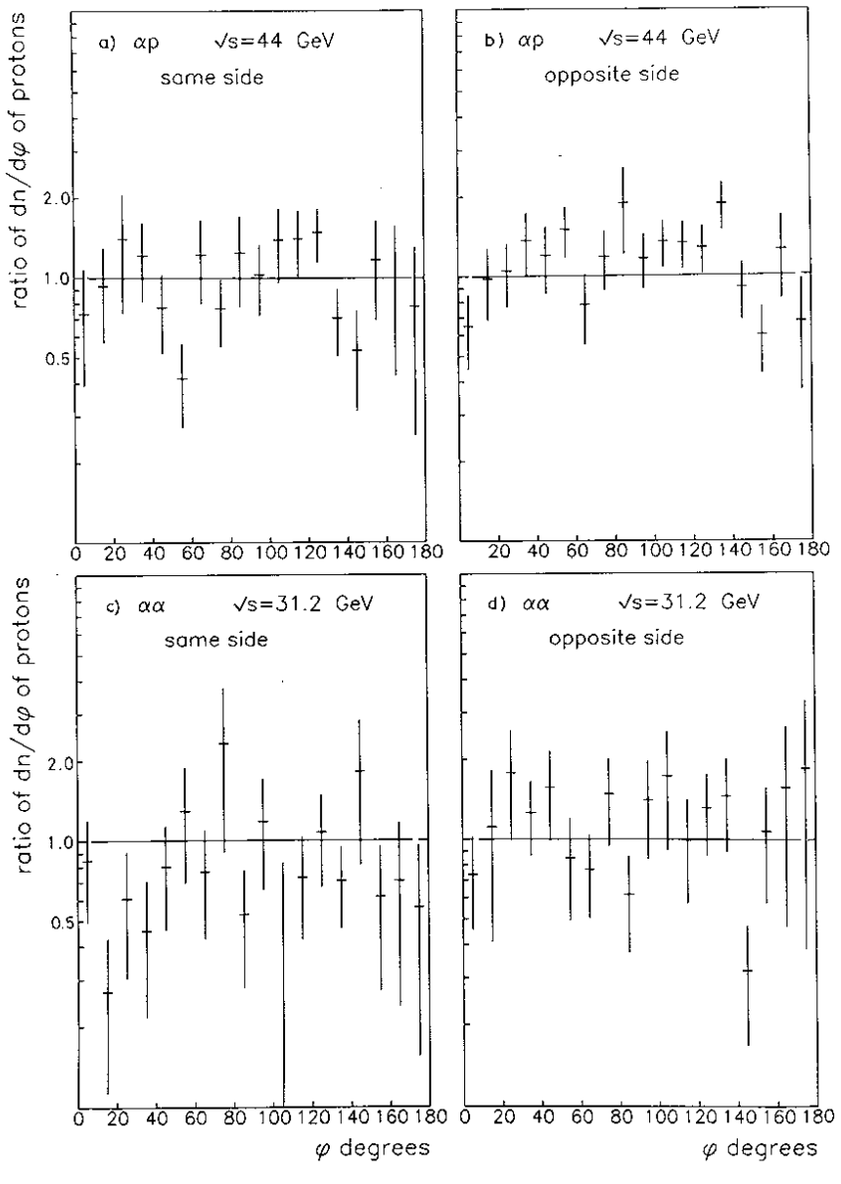
a) αp √s=44 GeV
same side
b) αp √s=44 GeV
opposite side
c) αα √s=31.2 GeV
same side
d) αα √s=31.2 GeV
opposite side
ratio of dn/dφ of protons
φ degrees
φ degrees

Fig. 5

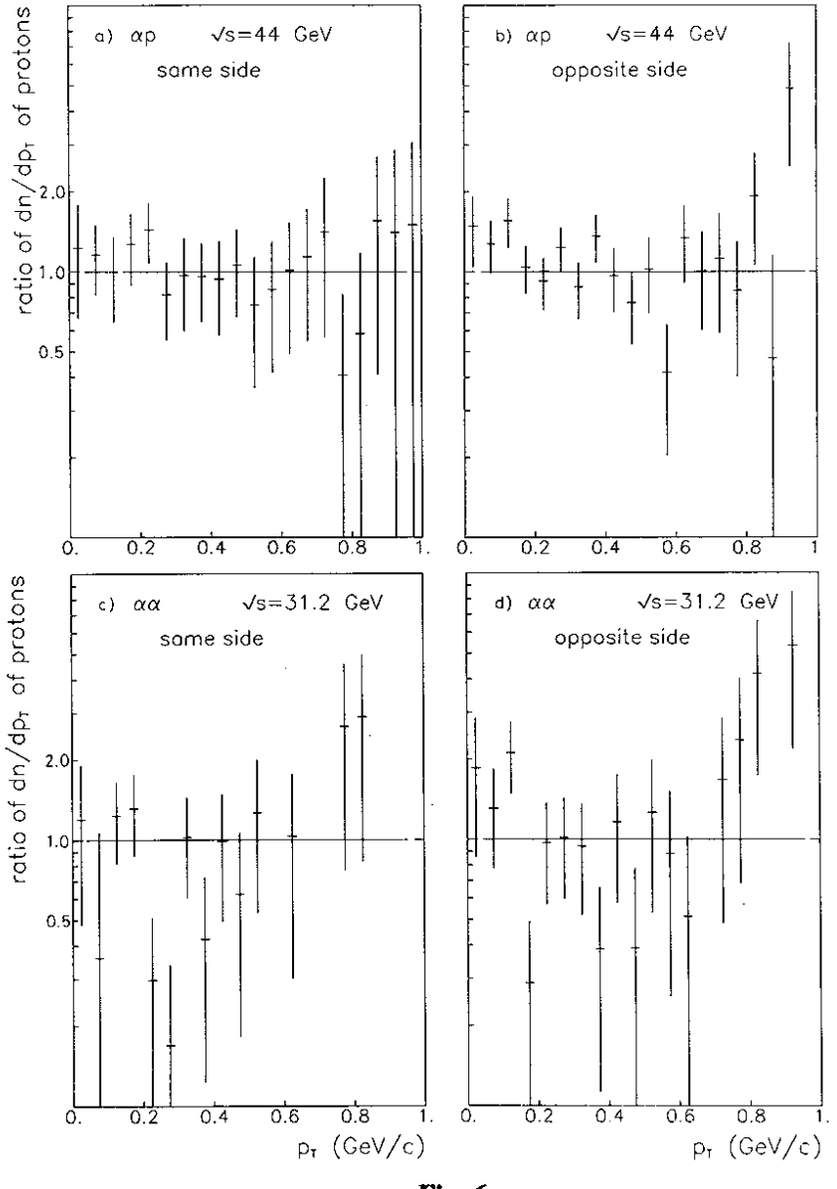
a) αp √s=44 GeV
same side
b) αp √s=44 GeV
opposite side
c) αα √s=31.2 GeV
same side
d) αα √s=31.2 GeV
opposite side
ratio of dn/dpT of protons
pT (GeV/c)
pT (GeV/c)

Fig. 6